ELSEVIER

Journal of Nuclear Materials 300 (2002) 127–140

journal of nuclear materials

www.elsevier.com/locate/jnucmat

Comparison of microstructural features of radiation embrittlement of VVER-440 and VVER-1000 reactor pressure vessel steels

E.A. Kuleshova *, B.A. Gurovich, Ya.I. Shtrombakh, D.Yu. Erak, O.V. Lavrenchuk

Russian Research Center 'Kurchatov Institute', Kurchatov Sq. 1, Moscow 12312, Russia

Received 11 June 2001; accepted 13 November 2001

Abstract

Comparative microstructural studies of both surveillance specimens and reactor pressure vessel (RPV) materials of VVER-440 and VVER-1000 light water reactor systems have been carried out, following irradiation to different fast neutron fluences and of the heat treatment for extended periods at the operating temperatures. It is shown that there are several microstructural features in the radiation embrittlement of VVER-1000 steels compared to VVER-440 RPV steels that can cause changes in the contributions of different radiation embrittlement mechanisms for VVER-1000 steel. © 2002 Published by Elsevier Science B.V.

1. Introduction

It is well established that neutron irradiation of reactor pressure vessel (RPV) steels results in radiation embrittlement, which can be measured on an upward shift in the ductile–brittle transition temperature (DBTT) and a drop in upper shelf toughness of impact energy in Charpy V-notch impact tests [1,2].

The radiation embrittlement rates of the welds of the old VVER-440 RPVs did not allow their safe operation during design service life without additional measures (recovery annealing of the RPV in the holt line region). High radiation embrittlement rates of these materials was caused by high phosphorous and copper content in the steels.

Therefore, the content of these impurity elements was essentially reduced in VVER-1000 RPV materials. However, during manufacturing of VVER-1000 RPV steels, the nickel content was raised to enhance their workability, especially in RPV welds, compared with VVER-440 materials.

Despite low phosphorous and copper contents in VVER-1000 RPV steels, the results of studies of these materials based on the first surveillance specimens (SS) sets have revealed a high embrittlement rate of steel with high nickel content compared with predicted embrittlement determined from the Russian Guide [3].

An understanding of the radiation embrittlement mechanisms of RPV steels allows predictions to be made of materials behavior after long-term operation. Now the response of VVER-440 RPV steels for primary (i.e. before annealing) irradiation conditions is well known for a wide spectrum of fast neutron fluences for the design operation period and beyond. Studies of microstructural features in VVER-1000 RPV steels after irradiation can improve the prediction of their irradiation embrittlement behavior for further operation.

With regard to radiation embrittlement mechanisms, it is necessary to understand that together with hardening

* Corresponding author.

0022-3115/02/$ - see front matter © 2002 Published by Elsevier Science B.V.
PII: S0022-3115(01)00752-8

an essential contribution to radiation embrittlement is the occurrence of solute segregation (primarily phosphorous), to interface boundaries of precipitates (including those that arise during irradiation for example, on copper-enriched precipitates or copper-vacancy clusters) [4–6].

It is expected that the fracture surfaces of impact-test specimens, tested at different and comparable temperatures before and after irradiation, contains direct information about the mechanisms responsible for radiation embrittlement of RPV steels. It is known that steels with body centered cubic lattice (including pressure vessel steels) are in most cases used in such conditions of finishing heat treatment, which, as a rule, designed to avoid the occurrence of temper brittleness. Under these conditions the fracture surfaces of unirradiated specimens from RPV steels are different combinations of zones with ductile dimple fracture mode and also zones with quasi-cleavage and cleavage fracture modes [7]. In the simplest case, when radiation embrittlement of steels is caused only by dispersed barrier hardening, irradiation should not result in any new types of fracture mode of impact-test specimens. In reality, when several simultaneous mechanisms influence on RPV steel radiation embrittlement and which include the formation of intergranular and intragranular solute segregation under irradiation, then brittle and ductile intergranular fracture modes can occur in specimens [6,8].

A comparison of the results of microstructural studies of RPV steels VVER-440 and VVER-1000 reactor systems that differ principally in basic alloying elements (first of all nickel) content and also in impurity elements content (first of all phosphorous and copper), could give a more complete understanding of the mechanisms responsible for RPV steels radiation embrittlement.

2. Materials and test methods

The following steels were studied:

- 15Kh2MFA: This is the base metal of the VVER-440. After forging the following heat treatment was applied: 1000 °C, 10 h hold → cooling in oil; tempering at a temperature of 700 °C for 16 h → air cooling.
- Sv-10KhMFT: This is the weld metal of the VVER-440. After welding the following heat treatment was applied: tempering at a temperature of 665 °C, for 15 h → furnace cooling to 300 °C, then air cooling.
- 25Kh3NM: This is the base metal of an experimental reactor of the VVER type. After forging the following heat treatment was applied: 870–890 °C, air cooling down to 700–800 °C, then cooling in oil; tempering at a temperature of 620–670 °C then furnace cooling.
- 15Kh2NMFAA: This is the base metal of the VVER-1000. After forging the following heat treatment was applied: austenization at a temperature of 920 °C for 1 h, then water cooling; annealing at a temperature of 650 °C, air cooling; annealing at a temperature of 620 °C for 25 h, annealing at a temperature of 650 °C for 20 h, final furnace cooling to room temperature.
- Sv-10KhGNMAA: This is the weld metal of the VVER-1000. After welding the following heat treatment was applied: tempering at a temperature of 610–620 °C for 5 h, furnace cooling to 400 °C, then air cooling.

The chemical composition of RPV steels studied are given in Table 1.

The embrittlement of specimens after irradiation was estimated by DBT temperature shift and also by the lowering of the upper shelf (US) energy level on the temperature dependence curve for Charpy-V impact tests.

Broken halves of Charpy specimens were studied using fractography. To preserve their fracture surfaces they were selected and stored in vacuum immediately after testing.

The fracture surfaces were studied using an X-ray micro analyzer SXR-50 modified for radioactive examination ('Cameca' Co., France), and placed in a hot cell. Fracture images were obtained using secondary electrons at an accelerating voltage of 20 kV and a probe current of 0.8 nA in the magnification range 50–3500. The percentage of different fracture modes (ductile, brittle intergranular, ductile intergranular, cleavage and quasi-cleavage) in the total fracture surface after testing at different temperatures was estimated by Glagolev's method [9]. The absolute error of measuring at confidence level of 95% did not exceed 5%. The test temperatures for each material corresponded to: upper shelf (US); ductile-to-brittle transition temperature (DBTT) and lower shelf (LS) on the impact strength temperature dependence curve.

Transmission electron microscopy (TEM) studies were carried out using an electron microscope TEM-SCAN-200CX ('Jeol', Japan) at an accelerating voltage of 200 KV. The density of radiation defects and precipitates were estimated with a foil thickness measured using a convergent beam electron diffraction method [10], that provides an accuracy with errors less than 5%. The specimens for TEM-studies were cut out from the broken halves of Charpy specimens. Further preparation of specimens included electropolishing using a 'Struers' installation (Austria) at a temperature of −60 to −70 °C just before placing them in the microscope. The electrolyte composition for electropolishing was 10% $HClO_4$ + 90% methanol.

Table 1
Chemical composition of pressure vessel materials

Steel type	Weight%								
	Si	Mn	P	S	Cu	Ni	Cr	Mo	C	V
15Ch2MFA base metal VVER-440	0.27–0.37	0.39–0.48	0.009–0.0375	0.012–0.018	0.09–0.17	0.19–0.27	2.52–3.00	0.64–0.71	0.13–0.18	0.25–0.31
SV-10ChMFT weld metal VVER-440	0.15–0.35	0.97–1.03	0.018–0.039	0.012–0.013	0.15–0.21	0.09–0.29	1.37–1.58	0.43–0.50	0.05–0.07	0.19–0.23
25Ch3NM base metal experimental reactor	0.44	0.49	0.024	0.018	0.10	1.02	3.03	0.40	0.23	–
15Ch2NMFA base metal VVER-1000	0.17–0.37	0.3–0.6	0.029–0.036	0.012–0.013	0.07–0.08	1.1–1.22	1.8–2.1	0.55–0.7	0.13–0.18	0.10–0.12
SV-10ChGNMAA weld metal VVER-1000	0.14–0.41	0.72–0.94	0.010–0.011	0.006–0.012	0.05–0.08	1.17–1.88	1.70–1.88	0.55–0.70	0.05–0.12	0.01–0.03

3. Results

3.1. Fractographic studies

The results of fractographic studies of broken Charpy halves of VVER-440 and VVER-1000 RPV steels in the initial condition, after different irradiations and also after isothermal ageing at the operating temperatures are given in Table 2. The temperatures of impact tests, absorbed energy values for specific specimens and values of the DBTTs are also given in this table.

The following observations, concerning features of impact-test specimen fractures of VVER-1000 steels in comparison with similar specimens of VVER-440 steels can be made.

(1) Irradiation of VVER-440 and VVER-1000 steels under conditions of RPV operation causes significant changes in the fracture mode of impact-test specimens in comparison with unirradiated specimens at comparable test temperatures. Thus, in fractures of specimens tested in the temperature range of the upper shelf, in addition to zones with ductile, dimple character fracture, there are zones with a ductile intergranular fracture mode (Fig. 1(a)). Their fraction in total fracture surface reaches 10–15% in specimens of VVER-440 steels and does not exceed 5–10% in specimens of VVER-1000 (see Table 2). Such zones can occur in fractures in the case, when grain boundaries are decorated by precipitates with phosphorous segregation on interface boundaries of these precipitates caused by heat treatment or irradiation (i.e. intragranular segregation).

(2) At lower test temperatures close to the transition temperature, a noticeable reduction of ductile and ductile-intergranular fracture zones in the total fracture surface of irradiated specimens is detected. Significant number of transcrystalline fracture regions also occurs by cleavage and quasi-cleavage modes. It is necessary to note, that in Charpy specimens of VVER-440 base metal and also in VVER-1000 base and weld metals irradiation induces a brittle intergranular fracture mode in a noticeable number of regions (Fig. 1(b) and (c)). Their fraction usually is 15–30% of the total fracture surface (Table 2). However, for some steels it could be 65–70% (Table 2). The occurrence of a brittle intergranular fracture mode indicates the occurrence of intergranular phosphorous segregation.

(3) At lower impact test temperatures to values corresponding to the lower shelf, there is practically a complete absence of regions with a ductile and ductile-intergranular fracture mode in specimen fractures (Table 2). Simultaneously there is some decrease of regions with intergranular fracture mode (in those materials, where they were) in total fracture surface (Table 2). In contrast to the above, the fraction of zones with quasi-cleavage and/or cleavage fracture modes is increased (Table 2).

Table 2
Summary data of fractographic analysis results for investigated Charpy specimens

N	Material (wt%)	Specimen types	NPP unit	Fluence $\times 10^{23}$ (n m^{-2})	Condition	Test temperature (°C)	DBTT, T_k (°C)	Absorbtion energy, *J*	Point on the curve KCV-T	Quota of different fracture modes (%)				
										Ductile	Quasi-cleavage	Cleavage	Intergranular	Ductile intergranular
1	25Kh3NM	BM Charpy	Cover from experimental PWR	–	Unirradiated, heat influence 60 000 h	−150	−22	5.4	LS	–	35	–	65	–
2	P = 0.018					−35		46	DBT	10	5	5	65	15
3	Cu = 0.10					100		191	US	85	–	–	–	15
4	25Kh3NM	BM Charpy	Trepan from experimental PWR	1.6	Irradiated	0	107	18	LS	10	15	10	65	–
5	P = 0.018					113		47	DBT	35	10	–	45	10
6	Cu = 0.10					200		108	US	90	–	–	–	10
7	15Kh2MFA	BM Charpy	Trepan from WWER-440	–	Unirradiated	−75	−55	9	LS	–	90	–	10	–
8	P = 0.012					−37.5		13	DBT	10	80	5	15	–
9	Cu = 0.09					−25		173	DBT	95	–	5	–	5
10	15Kh2MFA	BM Charpy	Trepan from WWER-440	1.5	Irradiated	−50	15	4	LS	–	65	5	30	–
11	P = 0.012					12		47	DBT	25	40	–	35	–
12	Cu = 0.09					100		188	US	90	–	–	–	10
13	Sv-10KhMFT	WM Charpy	Trepan from WWER-440	–	Unirradiated	−25	10	22	LS	20	55	25	–	–
14	P = 0.031					12.5		54	DBT	40	35	20	–	5
15	Cu = 0.24					160		133	US	90	–	–	–	10
16	Sv-10KhMFT	WM Charpy	Trepan from WWER-440	1.6	Irradiated	125	165	19	LS	20	70	10	–	–

17	P = 0.031					188		54	DBT	55	25	15	–	5
18	Cu = 0.24					225		84	US	85	–	–	–	15
19	15Kh2NMFA	BM Charpy	Surveillance samples for WWER-1000	–	Unirradiated, heat influence 42,360 h	−100	−67	7	LS	–	80	20	–	–
20	P = 0.04					−56		166	DBT	65	20	15	–	–
21	Cu = 0.04, Ni = 1.1					100		248	US	100	–	–	–	Traces
22	15Kh2NMFA	BM Charpy	Surveillance samples	1.6	Irradiated	−100	−45	3.5	LS	–	55	45	–	–
23	P = 0.04					−44		137	DBT	50	30	20	–	–
24	Cu = 0.04, Ni = 1.1					100		211	US	95	–	–	–	5
25	15Kh2NMFA	BM Charpy	Surveillance samples for WWER-1000	–	Unirradiated	−75	−74	40	DBT	20	50	30	Traces	–
26	P = 0.08													
27	Cu = 0.07, Ni = 1.22													
28	15Kh2NMFA	BM Charpy	Surveillance samples for WWER-1000	–	Unirradiated, heat influence 30,360 h	−150	−70	4	LS	Traces	65	35	–	–
29	P = 0.08					−75		86	DBT	35	35	25	Traces	–
30	Cu = 0.07, Ni = 1.22					175		238	US	95	–	–	–	5
31	15Kh2NMFA	BM Charpy	Surveillance samples for WWER-1000	1.6	Irradiated	−62.5	−50	58	DBT	30	50	15	5	–
32	P = 0.08					−37.5		83	DBT	40	35	15	10	–

(*continued on next page*)

Table 2 (*continued*)

N	Material (wt%)	Specimen types	NPP unit	Fluence $\times 10^{23}$ (n m^{-2})	Condition	Test temperature (°C)	DBTT, T_k (°C)	Absorbtion energy, *J*	Point on the curve KCV-T	Quota of different fracture modes (%)				
										Ductile	Quasi-cleavage	Cleavage	Intergranular	Ductile intergranular
33	Cu = 0.07, Ni = 1.22					23		202	US	80	–	–	–	10
34	SV10KhGN-MAA	WM Charpy	Surveillance samples for WWER-1000	–	Unirradiated	−37.5	−49	38	DBT	25	50	10	15	–
35	P = 0.07					−25		69	DBT	55	25	10	10	Traces
36	Cu = 0.05, Ni = 1.57													
37	SV10KhGN-MAA	WM Charpy	Surveillance samples for WWER-1000	–	Unirradiated, heat influence 30,360 h	−140	−35	3.5	LS	Traces	75	15	10	–
38	P = 0.07					−25		45	DBT	30	45	10	15	–
39	Cu = 0.05, Ni = 1.57					175		157	US	100	–	–	–	–
40	SV10KhGN-MAA	WM Charpy	Surveillance samples for WWER-1000	1.3	Irradiated	−100	4	3	LS	5	80	15	Traces	–
41	P = 0.07					0		51	DBT	40	25	15	20	–
42	Cu = 0.05, Ni = 1.57					150		122	US	95	–	–	–	5
43	SV10KhGN-MAA	WM Charpy	Surveillance samples for WWER-1000	–	Unirradiated, heat influence 42,360 h	−100	0	2.5	LS	5	60	15	20	–

44	P = 0.09				12.5		61.5	DBT	50	35	10	5	–
45	Cu = 0.02, Ni = 1.88				175		108	US	100	–	–	–	Traces
46	SV10KhGN-MAA	WM Charpy	Surveil-lance samples for WWER-1000	1.6	Irradi-ated	−50	40	7	LS	5	50	15	30	–
47	P = 0.09					50		61	DBT	60	15	10	15	–
48	Cu = 0.02, Ni = 1.88					175		108	US	100	–	–	–	Traces

BM—base metal; WM—weld metal; LS—lower shelf; DBT—ductile-to-brittle transition region; US—upper shelf.

(4) Some experimental data shows (Table 2), that long heat treatments (30,000–60,000 h) of RPV steels without irradiation at temperature of 270–290 °C can also cause the formation of intergranular phosphorous segregation. For this conditions, the fraction of zones with brittle intergranular fracture mode in fractures of Charpy specimens from experimental reactor steel reaches 65–70% (Table 2). For impact-test specimens of the same steel after irradiation in the experimental RPV for a fast neutron fluence of 1.6×10^{23} n m^{-2} at the temperature of 270 °C the fraction of zones with brittle intergranular fracture mode was also 65–70% (Table 2). It should be noted that in experimental RPV material (where the content of both nickel and phosphorous was higher) this effect occurs more clear. Phosphorous segregation on the grain boundaries in VVER-1000 RPV steels at similar heat influences and small radiation doses results in smaller levels of brittle intergranular fraction of fracture.

Therefore, a comparative fractographic study of a wide spectrum of RPV steels (base metal and weld metal) in the initial condition and after irradiation has shown that main distinctive feature of impact-test specimen fracture surfaces in irradiated condition (and in some cases after long heat treatment), common for specimens of VVER-440 and VVER-1000 steels is transition from only transcrystalline fracture to mixed fracture mode with brittle and/or ductile intercrystalline fracture.

It should be noted that temperature interval of brittle intergranular fraction occurrence at testing is higher, the more is phosphorous content in VVER-440 steel and nickel content in VVER-1000 steel (at similar another elements content).

At the same time the fraction of zones with ductile intergranular fracture mode in specimens of any steel is not connected directly with phosphorous level in segregation on interface boundaries of corresponding precipitates. It is largely determined by share of grain boundaries surface that are decorated by such precipitates to total grain boundaries surface. It should be noted specially that brittle intergranular fracture in VVER-1000 steel specimens occurs at such low phosphorous content for which this fracture mode is absent in VVER-440 steel specimens.

The influence of phosphorous content on the fraction of brittle intergranular component is of complex character. Thus, in VVER-440 base metal specimens, where phosphorous content is significantly less than in VVER-440 weld metal, after irradiation there are zones with brittle intergranular fracture mode in Charpy specimens. At the same time the similar type of fracture was never seen earlier in Charpy specimens of VVER-440 weld metal. Presumably it is caused by differences in microstructure of these materials. According to the data [11], it might be pointed out that there is a possible reason for

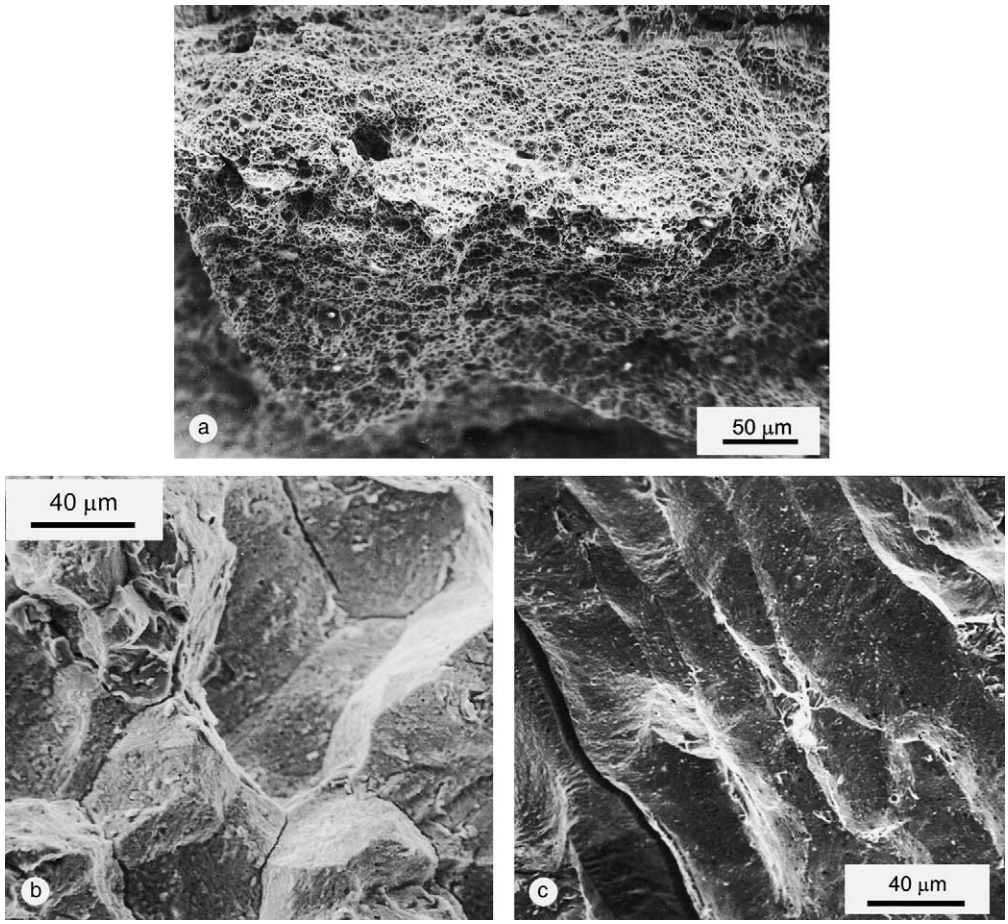

Fig. 1. Typical regions of intergranular fracture in irradiated impact specimens of pressure vessel steels: (a) ductile intergranular fracture, (b) brittle intergranular fracture of base metal and (c) brittle intergranular fracture of weld metal.

higher tendency of Charpy specimens from irradiated VVER-440 base metal to exhibit brittle intergranular fracture in comparison with similar Charpy specimens from irradiated VVER-440 weld metals. As metallographic examination has shown, the microstructure of the base metal is homogeneous and consists of tempered bainite (Fig. 2(a)). Compared to base metal, the grains of VVER-440 weld metal consist of tempered bainite and in locations of former high angle austenite grain boundaries there are also grains of excess alpha-ferrite without carbide segregation (Fig. 2(b)), where intergranular fracture of impact-test specimens occurred mainly. Alloying of steels with Mo and Mn results in a marked drop of phosphorous solubility in alpha-ferrite [11] and, accordingly, can cause decreasing of phosphorous segregation on high angle boundaries of the weld. At the same time at impact testing of Charpy specimens made from base and weld metals of VVER-1000 with identical homogeneous tempered bainite structure on section of former austenite grains (Fig. 2(c) and (d)), the occurrence of brittle intergranular fracture in Charpy specimens is of equal probability.

Our research also has shown, that definite grain structure in fracture promotes increasing of brittle intergranular fraction in tested Charpy specimens. It, first of all, concerns specimens from the welds of VVER-1000.

The grain structure of the welds (both VVER-440 and VVER-1000) consists of columnar grains (up to 5000 μm length), located fan-shaped along the heat removal direction during welding, and small (100–200 μm) equiaxial grains on the periphery of the columnar grains (see Fig. 3). The position of the notch in Charpy specimens (relatively the grains location) determines the size of grains along the direction of crack initiation in them, and also the fraction of brittle intergranular fracture and, accordingly, the DBTT. The effect of grain size on DBTT is known and described by the equation: $T_k = D \ln d^{1/2}$, where T_k is DBTT, d is grain size, D is a constant.

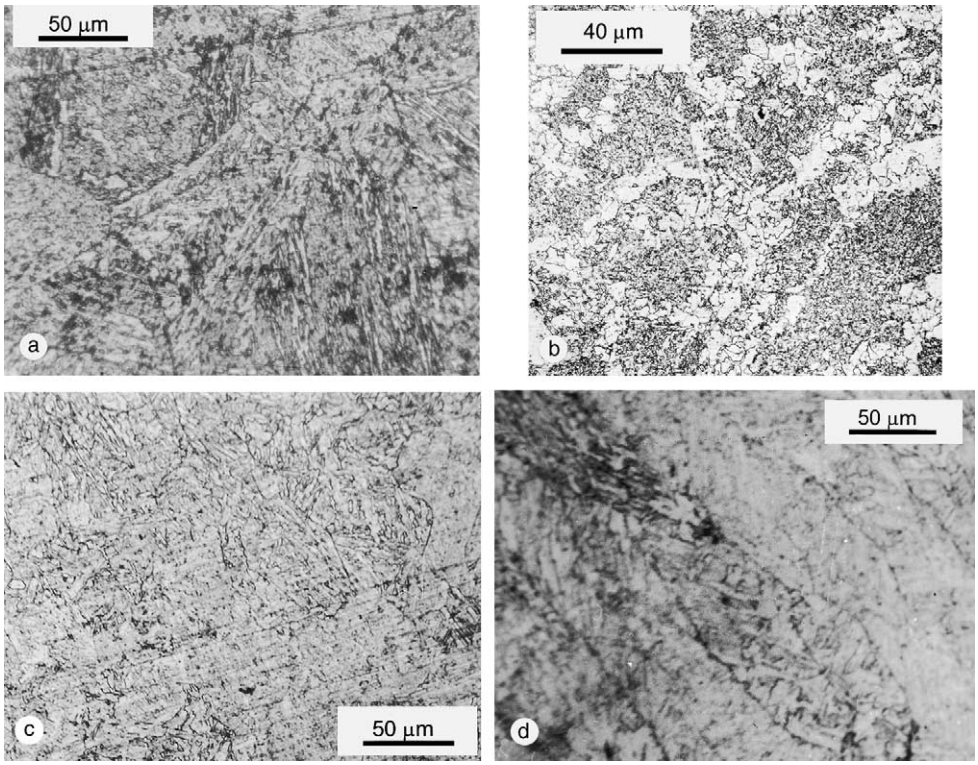

Fig. 2. Typical microstructure of power RPV steels: (a) base metal of VVER-440, (b) weld metal of VVER-440, (c) base metal of VVER-1000 and (d) weld metal of VVER-1000.

Fig. 3. Typical grain structure of the welds of VVER-440 and VVER-1000.

The results of a grain structure study of some broken Charpy specimens from the weld of VVER-1000 with portion of brittle intergranular fracture and DBTT is given in Table 3.

It should be noted that there is a temperature interval where the occurrence of brittle intergranular fracture is maximum in tested impact specimens. As a rule, it is the interval between the lower shelf and the DBTT. The results of grain structure study of tested Charpy specimens of VVER-1000 weld are given in Table 4. They clearly show that morphology and size of grains along crack propagation direction at impact testing influence essentially on both portion of brittle intergranular fracture and specimen absorbed energy. This effect is revealed clearly at testing of VVER-1000 weld with high nickel content.

3.2. Electron-microscopy studies

Typical results of TEM studies of VVER-440 and VVER-1000 RPV steels in the initial condition, after long heat treatment at operating temperatures and after irradiation in different conditions are given in Table 3. The results obtained allow a formulation of several common mechanisms and features of radiation-induced microstructural behavior under irradiation of materials of these two reactor types.

1. Irradiation causes occurrence of radiation defects (dislocation loops seen as 'black dots' (see Fig. 4(a)) in base and weld metals of both reactor types.
2. In addition there are disk precipitates (probably, vanadium carbides in VVER-440 and chromium carbides in VVER-1000) (see Fig. 4(b)). In VVER-440 RPV steels the density of disk-shaped precipitates increases under irradiation with increasing of fast neutron fluence, while in VVER-1000 RPV steels their density does not change under irradiation, i.e. disk-shaped precipitates in VVER-1000 RPV steels versus VVER-440 RPV steels are not radiation-induced

Table 3
Data on densities and average sizes of radiation defects, disk-shaped and rounded precipitates

No.	Condition	$n_{loops} \times 10^{15}$ (cm^{-3})	$\langle d \rangle_{loops}$ (nm)	$n_{disk} \times 10^{15}$ (cm^{-3})	$\langle d \rangle_{disk}$ (nm)	$n_{rounded} \times 10^{15}$ (cm^{-3})	$\langle d \rangle_{rounded}$ (nm)
Specimens from weld of VVER-440 ($P = 0.047\%$, $Cu = 0.10\%$, $C = 0.049\%$, $Ni = 0.22\%$)							
1	Unirradiated	–	–	0.5–0.6	20.4	–	–
2	Irradiated $F = 2.4 \times 10^{23}$ m^{-2} ($E \geqslant 0.5$ MeV)	5–6	3	30–50	9.5	500–700	2.0–3.0
Surveillance specimens from the weld of VVER-440 ($P = 0.039\%$, $Cu = 0.17\%$,, $C = 0.06\%$, $Ni = 0.19\%$)							
1	Unirradiated	–	–	0.7–0.8	22.8	–	–
2	Irradiated $F = 0.9 \times 10^{23}$ m^{-2} ($E \geqslant 0.5$ MeV)	2–3	5–6	20–25	18.7	1700–2000	2.0–2.5
Surveillance specimens from base metal of VVER-1000 ($P = 0.008\%$, $Cu = 0.04\%$, $C = 0.14\%$, $Ni = 1.1\%$)							
1	Unirradiated, heat influence 42,360 h	–	–	3–5	40	–	–
2	Irradiated $F = 2 \times 10^{23}$ m^{-2} ($E \geqslant 0.5$ MeV)	3–4	4–5	3–5	41	2–3	2–3
Surveillance specimens from base metal of VVER-1000 ($P = 0.008\%$, $Cu = 0.07\%$, $C = 0.15\%$, $Ni = 1.22\%$)							
1	Unirradiated, heat influence 30,360 h	–	–	3–5	25	–	–
2	Irradiated $F = 1.71 \times 10^{23}$ m^{-2} ($E \geqslant 0.5$ MeV)	10–12	7–8	3–5	25	2–3	4–5
Surveillance specimens from the weld of VVER-1000 (P = 0.009%, $Cu = 0.02\%$, $C = 0.05\%$, $Ni = 1.88\%$)							
1	Unirradiated, heat influence 42,360 h	–	–	0.3–0.5	43	–	–
2	Irradiated $F = 1.48 \times 10^{23}$ m^{-2} ($E \geqslant 0.5$ MeV)	4–5	4–5	0.3–0.5	42	–	–
Surveillance specimens from the weld of VVER-1000 ($P = 0.007\%$, $Cu = 0.05\%$, $C = 0.06\%$, $Ni = 1.57\%$)							
1	Unirradiated, heat influence 30,360 h	–	–	0.3–0.5	33		–
2	Irradiated $F = 1.18 \times 10^{23}$ m^{-2} ($E \geqslant 0.5$ MeV)	3–4	4–5	0.3–0.5	32	2–3	4–5

Table 4
Fracture grain structure Charpy weld specimens for VVER-1000 Ni = 1.59 Cu = 0.05 P = 0.010, irradiated fluence 6.04×10^{23} n m^{-2}, $T_k = -21$ °C

Test temperature (°C)	Absorbtion energy, J	Portion of the brittle intergranular fracture	Grain type	Average size (μm)		Grain fracture on a fracture surface	
				Columnar	Equal axis	Columnar	Equal axis
−62.5	10	15	CG II, EA	300	500	0.5	0.5
−31	50	10	CG II, EA	250	500	0.5	0.5
−25	27	30	CG ∠, EA	1000	1200	0.7	0.3
−18	76	–	CG II	250	–	1	–
−12.5	67	5	EA	–	350	–	1
0	62	15	CG ∠, EA	500	500	0.5	0.5
75	136	–	CG II	250	–	1	–

EA—equal axises; CG—columnar grains; CG II—CG parallel to the surface with the notch; CG ∠—CG with the angle to the surface with the notch.

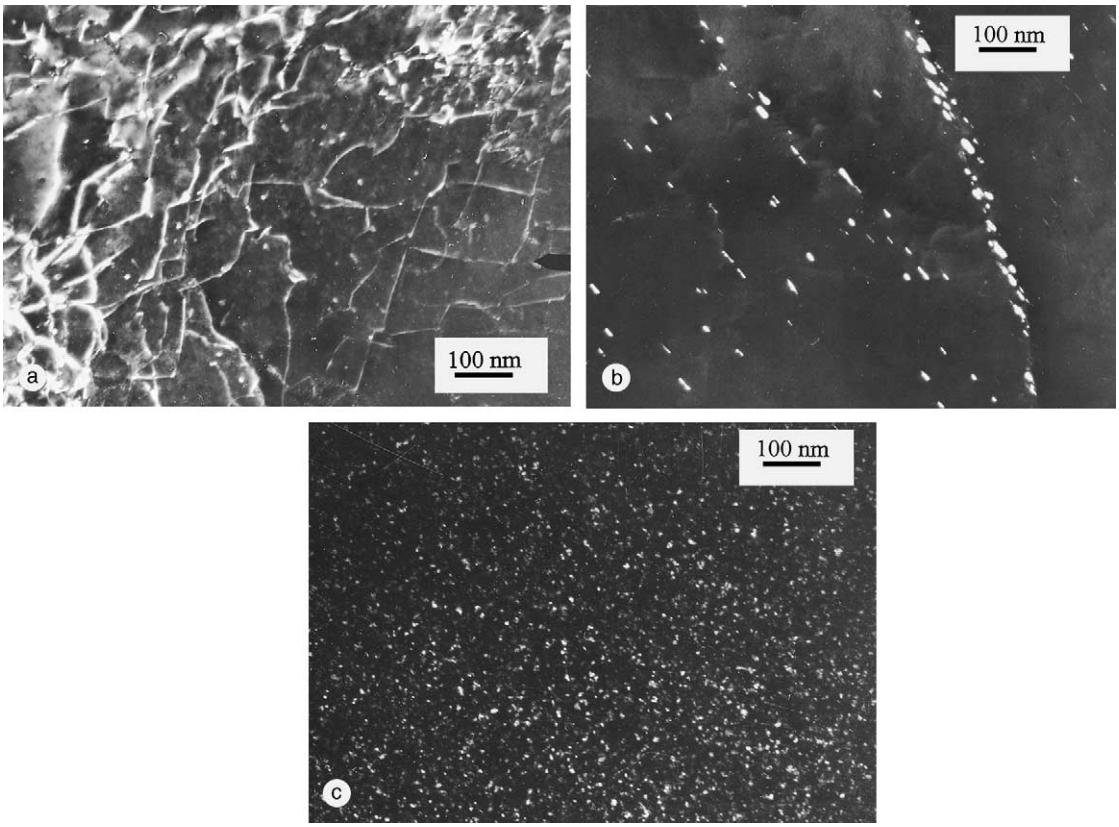

Fig. 4. Radiation-induced microstructural components of pressure vessel steels: (a) radiation defects—dislocation loops (black dots), (b) disk precipitates (carbides) inside and on boundaries of former austenite grains, (c) rounded precipitates (copper-enriched).

and determined only by the initial properties of materials.

3. In base and weld metals of both reactor types irradiation causes also the formation of rounded precipitates (copper-enriched) (Fig. 4(c)). The much lower copper content in VVER-1000 RPV steels versus VVER-440 RPV steels is the reason for the much smaller density (10^2–10^3 times) of rounded precipitates in them. The rounded precipitates at copper content of 0.02% in VVER-1000 RPV steels are not detected by TEM methods (see Table 3).

4. Discussion and conclusion

The results obtained show, that irradiation of Russian RPV steels is accompanied by the following microstructural changes:

4.1. In VVER-440 RPV steels

- Occurrence of radiation defects – dislocation loops.
- Essential increase in the density of disk-shaped precipitates and the formation of many rounded precipitates. The first are presumed to be vanadium carbides and the second are copper-enriched precipitates.
- Initiation of intergranular and intragranular solute (principally phosphorous) segregation, that are seen in fractures of tested impact specimens as brittle and ductile intergranular fractures, respectively. At this in fracture surface portion of brittle intergranular fracture can reach 30%, and portion of ductile intergranular fracture – 15% at high phosphorous content (up to 0.05%).

4.2. In VVER-1000 RPV steels

- Occurrence of radiation defects – dislocation loops.
- Increase in the density of rounded precipitates (presumably copper-enriched) but a constant density of disk-sharped precipitates (presumably chromium carbides). At similar values of fast neutron fluence the density of radiation-induced precipitates in VVER-1000 RPV steels in 10^2–10^3 times lower than their density in VVER-440 RPV steels.
- Initiation of intergranular solute (principally phosphorous) segregation. At this portion of the brittle intergranular fracture could be 30% and more in tested Charpy specimens caused by segregation formation at low phosphorous content values (less than 0.011%). Portion of ductile intergranular fracture caused by formation of intragranular impurities segregation on the interphase boundary of radiation-induced precipitates, located on former austenite grains does not exceed 5–10%.

The authors considered earlier in detail different mechanisms and their relative contribution to RPV steels radiation embrittlement (i.e. in DBTT shift estimated at impact tests) [6]. At this there was shown that radiation embrittlement is stipulated, first of all, by formation of intragranular phosphorous segregation and in lesser degree by complex of effects, which it is accepted to name shortly as irradiation hardening. Intergranular phosphorous segregation contribution in radiation embrittlement of RPV steels was evaluated as not more than 10–20%. The basic data file, that was the base for evaluation of different mechanisms relative contribution to RPV steels radiation embrittlement, mainly referred to VVER-440 materials with high phosphorous (up to 0.05%) content and low nickel content (less than 0.3%).

It should be said that in the works devoted to steels temper brittleness, the tendency to formation of intergranular phosphorous segregation at increasing of nickel content was noted [12]. The experimental data shows that long heat exposition (30 000–60 000 h) without irradiation of RPV steels with high nickel content at a temperature of 270–290 °C causes the formation of intergranular phosphorous segregation and, as a consequence, occurrence of regions with brittle intergranular fracture mode. For these conditions the fraction of regions with brittle intergranular fracture mode in Charpy specimen fractures in some cases can reach 65% (see Table 2). For impact-test specimens of the same steel after irradiation to different fast neutron fluences at a temperature of 270–290 °C the fraction of regions with brittle intergranular fracture mode also can reach 65–70% (see Table 2). These data show that formation of intergranular phosphorous segregation in RPV steels during long time largely depends on parameters of heat treatment, as at developing of temper brittleness. Thereby it is possible to assume that in RPV steels with high nickel content (for example, in VVER-1000 RPV materials) the contribution of temper embrittlement mechanism to final effect of formation of intergranular phosphorous segregation under irradiation will be higher. Therefore, comparative results, obtained in this work, of complex microstructural and fractographic studies allow one to improve and understand more definitely how the above mentioned mechanisms are implemented and caused together radiation embrittlement of VVER-1000 RPV steels.

It was shown earlier [6,8,13] that for occurrence of intragranular phosphorous segregation, beside phosphorous, there are necessary precipitates with tendency to phosphorous segregation formation on their interphase boundaries. Such precipitates could be in RPV steels before irradiation. But these precipitates will occur much more during irradiation. Their formation is, first of all, the result of the fact that at pressure vessel manufacturing there is fixed content of some impurity elements (for example, copper) in the steel matrix, considerably higher than their equilibrium solubility at RPV operating temperatures. As it is shown above, precipitates, on which boundaries phosphorous can segregate, are disk-shaped (carbides) and rounded (copper-enriched) precipitates. In VVER-440 steels both types of precipitates are radiation-induced, i.e. their density essentially increases under irradiation with fast neutron fluence growth. In VVER-1000 steels only rounded, copper-enriched precipitates are radiation-induced, and the density of carbide disk-shaped pre-

cipitates under irradiation remains constant (see Table 3). At this (owing to much lower copper content in VVER-1000 RPV steels versus VVER-440 RPV steels) the density of rounded precipitates in 10^2–10^3 times less than density of rounded precipitates in VVER-440 RPV steels (see Table 3). Hence, essential lowering of radiation-induced precipitates (rounded) density and constant density of disk-shaped precipitates should result in decreasing of relative contribution of the mechanism of intragranular segregation formation in VVER-1000 RPV steels radiation embrittlement.

The density of radiation-induced rounded precipitates in the irradiated welds of VVER-1000 is comparable with density of radiation defects in them, and their average size is a little lower (see Table 3). For this reason radiation defects can contribute a little more to irradiation hardening of VVER-1000 RPV steels, than copper precipitates. The welds of VVER-1000 differ from the welds VVER-440: in VVER-440 materials the density of rounded precipitates is much higher than the density of radiation defects and, accordingly, contribution of rounded precipitates to lattice irradiation hardening is higher.

Therefore, comparative microstructural studies of pressure vessel steels of VVER-440 and VVER-1000 reactors, shown in this work, allow the following differences of embrittlement mechanisms in VVER-1000 RPV steels to be established. High nickel and low copper contents in VVER-1000 RPV steels in comparison with VVER-440 RPV steels could change the relative contribution of different mechanisms to radiation embrittlement of VVER-1000 RPV steels. At this contribution of the mechanism of intragranular solute (mainly phosphorous) segregation formation becomes less significant. The role of the mechanism of intergranular segregation formation (at definite phosphorous content of about 0.010%) grows. The third mechanism of radiation embrittlement is irradiation hardening, that is caused more by increasing of radiation defects density with increase in fast neutron fluence than by increasing density of copper-enriched precipitates. The contribution of this mechanism to radiation embrittlement of VVER-1000 RPV steels can be estimated at structure study of the specimens, irradiated up to higher fluence values.

Therefore, radiation embrittlement of VVER-1000 RPV steels at the first stages of irradiation is caused mainly by intergranular phosphorous segregation and metallurgical history in material structure, that can give in spread in data of impact tests. With increase in fast neutron fluence it should be expected in VVER-1000 RPV steel specimens further increase of radiation embrittlement, connected with density growth of radiation-induced defects.

However conclusions made on the basis of microstructural studies and shown in this work are only of a qualitative character. For quantitative estimation of the relative contribution of the three mechanisms responsible for radiation embrittlement of VVER-1000 RPV steels (formation of intergranular and intragranular impurities segregation, and irradiation hardening caused by formation of radiation defects and radiation-induced precipitates) it is necessary to carry out comprehensive testing and microstructural studies of impact-test and tensile specimens from RPV steels for a wide spectrum of nickel, copper and phosphorous contents in the initial condition, after irradiation to different fast neutron fluences, and also after different heat treatments and recovery annealing.

Acknowledgements

The work was carried out at Reactor Material Division support of RNC 'Kurchatov Institute' within the scope of basic research. The authors appreciate Division executives P.A. Platonov, Yu.A. Nikolaev, Yu.N. Korolev, K.E. Prihodko, V.N. Nevzorov and E.A. Krasikov for their useful advice and help in the work.

References

[1] N.N. Alekseenko, A.D. Amaev, I.B. Gorinin, V.A. Nikolaev, Radiation Damage of VVER Reactors Pressure Steel, Energoatomizdat, Moscow, 1981.
[2] J.R. Hawthorne, in: C.L. Briant, S.K. Bunerji (Eds.), Treatise on Materials Science and Technology, vol. 25, Academic Press, New York, 1983 (Chapter 10).
[3] PNAE-G-7-002-086, Energoatomizdat, NGA-01-85-1, NIKIET, 1989.
[4] R.J. McElroy, C.A. English, A.J. Foreman, et al., Effects of radiation on materials, in: R.K. Nanstad, M.L. Hamilton, F.A. Garner, A.S. Kumar (Eds.), 18th International Symposium, ASTM STP 1325, 1999, p. 296.
[5] R.B. Jones, J.T. Buswell, in: Proc. 3rd Int. Symp. on Environmental Degradation of Materials in Nuclear Power Systems—Water Reactors, Met. Society, USA, 1988, p. 111.
[6] B.A. Gurovich, E.A. Kuleshova, Yu.A. Nikolaev, Ya.I. Shtrombakh, J. Nucl. Mater. 246 (1997) 91.
[7] B.A. Gurovich, E.A. Kuleshova, O.V. Lavrenchuk, J. Nucl. Mater. 228 (1996) 330.
[8] B.A. Gurovich, E.A. Kuleshova, Ya.I. Shtrombakh, O.O. Zabusov, E.A. Krasikov, J. Nucl. Mater. 279 (2–3) (2000) 59.
[9] S.A. Saltykov, Stereometric Metallograph, Metallurgy, Moscow, 1976.
[10] P.M. Kelly, A. Jostsons, R.G. Blake, J.G. Napier, Phys. Status Solidi 31 (1975) 771.
[11] I.I. Novikov, The Theory of Metal Heat Treatment, Metallurgy, Moscow, 1978, p. 392.

[12] L.M. Utevskii, Ye.E. Glikman, G.S. Kark, Convertible Temper Brittleness in Steels and Iron Alloys, Metallurgy, Moscow, 1987, p. 222.

[13] B.A. Gurovich, E.A. Kuleshova, K.E. Prihodko, O.V. Lavrenchuk, Ya.I. Shtrombakh, J. Nucl. Mater. 264 (1998) 333.